Science World Journal Vol. 19(No 3) 2024 https://dx.doi.org/10.4314/swj.v19i3.26
www.scienceworldjournal.org
ISSN: 1597-6343 (Online), ISSN: 2756-391X (Print)
Published by Faculty of Science, Kaduna State University

AB-INITIO STUDY OF STRUCTURAL, ELECTRONIC, AND PHONON DISPERSION PROPERTIES OF V_2PbC MAX PHASE

*S.T. Ahams, J.S. Madugu

Department of Pure and Applied Physics, Adamawa State University, Mubi

*Corresponding Author Email Address: ahams112@adsu.edu.ng

ABSTRACT
Density functional theory calculations have been used to investigate the structural, electronic, and phonon dispersion properties of the V_2PbC MAX phase. The materials space group remains unaltered after variable cells have been relaxed. Computed phonon results show that V_2PbC is ductile and anisotropic. The electronic bands and density of states show metallic behaviour with impacts at and around the Fermi energy level originating mostly from the V-3D, Pb-6P, and C-2P orbitals. A set of phonon frequencies has been obtained by analyzing the forces connected to a systematic set of displacements. All phonon branches are positive, indicating that V_2PbC is dynamically stable.

Keywords: Density Functional Theory; MAX phase; ductile; electronic properties; phonon dispersion.

INTRODUCTION

Nanolamellar Carbides and Nitrides also known as 'MAX phases' are dual behaviour compounds with general stoichiometry $M_{n+1}AX_n$ $(n = 1 - 3)$. They are mostly high anisotropy materials that stir the interest of the scientific community either for their intrinsic physical properties(Bouhemadou, 2008, 2009a; Gupta et al., 2006; Yang et al., 2017) or as precursors of a new family of two-dimensional materials called MXenes(Khazaei et al., 2013, 2014; Li et al., 2016; Zhan et al., 2020). The latter is obtained by exfoliation of the former (Khazaei et al., 2013, 2017; Recent Advances in MXene Preparation Properties, 2015). M is a transition metal; A belongs to groups 13–16 and X is either C or N. New members of the MAX phase family are continuously being synthesized(Anasori et al., 2015; Barsoum, 2014; Bouhemadou, 2010; Wu et al., 2018). Pure MAX phases were synthesized for the first time in 1996(Eklund et al., 2010; Ingason et al., 2017; Istomin et al., 2016; Sobolev et al., 2017), but the absence of large single crystals has long prohibited a direct assessment of their physical anisotropies. Today, macroscopic crystals are available (Azzouz-Rached et al., 2021) and they have been used to probe magneto-transport (Dove, 2003) and electronic structures(Chlubny et al., 2015; Surucu et al., 2016). In this work, the lattice vibration anisotropies of V_2PbC MAX phase crystals have been calculated using thermo_pw (Dal Corso, 2016; Malica & Dal Corso, 2019). The atomic structure of MAX phases is peculiar because they combine in one system strong covalent $M = X$ bonds and weaker metallic $M = A$ bonds. Atomic masses may also be very different (C atoms are light in comparison with some M's and A's)(Qian et al., 2016). Analysis of the forces associated with a systematic set of displacements provides a series of phonon frequencies. To the best of our knowledge, phonon dispersion for V_2PbC has not yet been investigated theoretically and experimentally.

COMPUTATIONAL METHOD

Density Functional Theory (DFT) is a quantum mechanical instrument for calculating the ground state properties and electronic structures of solid materials and molecules(Payne et al., 1992). in this work calculations presented were achieved using the Quantum Espresso Package (QE) based on DFT. Exchange–correlation was treated within the generalized gradient approximation (GGA) of Perdew–Burke–Ernzerhof (PBE)(Perdew et al., 1996) with the plane-wave ultrasoft pseudopotential. The accuracy of calculations depends on two parameters, i.e., first, the kinetic energy cut-off, which determines the number of plane waves in the expansion, and second, the special k-points used for the Brillouin zone (BZ) integration. A plane wave cutoff energy was set at 500 eV, and the Monkhorst-pack scheme(Choudhary & Tavazza, 2019; H. J. M. and J. D. Pack, 1976; J. D. Pack & Monkhorst, 1977) of 10×10×8 k-points was employed. The ground state structural parameters were determined using the Broyden–Fletcher–Goldfarb–Shanno (BFGS)(Fischer & Almlöf, 1992) minimization technique while the convergence tolerance was set as follows: total energy tolerance less than 5×10^{-6} eV/atom, stress component less than 2×10^{-2} GPa, maximum force tolerance 1×10^{-2} eV/Å, and maximum displacement of the atom during the geometric optimization was less than 5×10^{-4} Å. The Debye temperature, mean, transverse, longitudinal sound velocities, and phonon dispersion were calculated from elastic constants using the thermo_pw package (Dal & Sissa, n.d.; Kucukbenli et al., 2014; Malica & Dal Corso, 2019).

RESULTS AND DISCUSSION

Structural Properties

The compound V_2PbC is a member of the 211 class of MAX phases and belongs to a P63/mmc space group symmetry which crystallizes in the hexagonal lattice. The crystal structure of a unit cell of V_2PbC is shown in Figure 2. There are 8 atoms in the unit cell which are: V(4), Pb(2), and C(2) located at the Wyckoff positions: V (0.33, 0.67, 0.08), Pb (0.67,0.33, 0.25) and C (0, 0, 0) respectively. At the initial step of our calculation, variable cells were fully relaxed, and final atomic coordinates were calculated. Full cutoff energy and k-points were converged and a structural optimization test, Figure 1 (a), (b), and (c) has been conducted for the material to determine the equilibrium structural parameters *a*(Å), *c*(Å), *c*/*a* and *V*(Å)^3 shown in Table **1** of minimum stable volume.

Science World Journal Vol. 19(No 3) 2024 https://dx.doi.org/10.4314/swj.v19i3.26
www.scienceworldjournal.org
ISSN: 1597-6343 (Online), ISSN: 2756-391X (Print)
Published by Faculty of Science, Kaduna State University

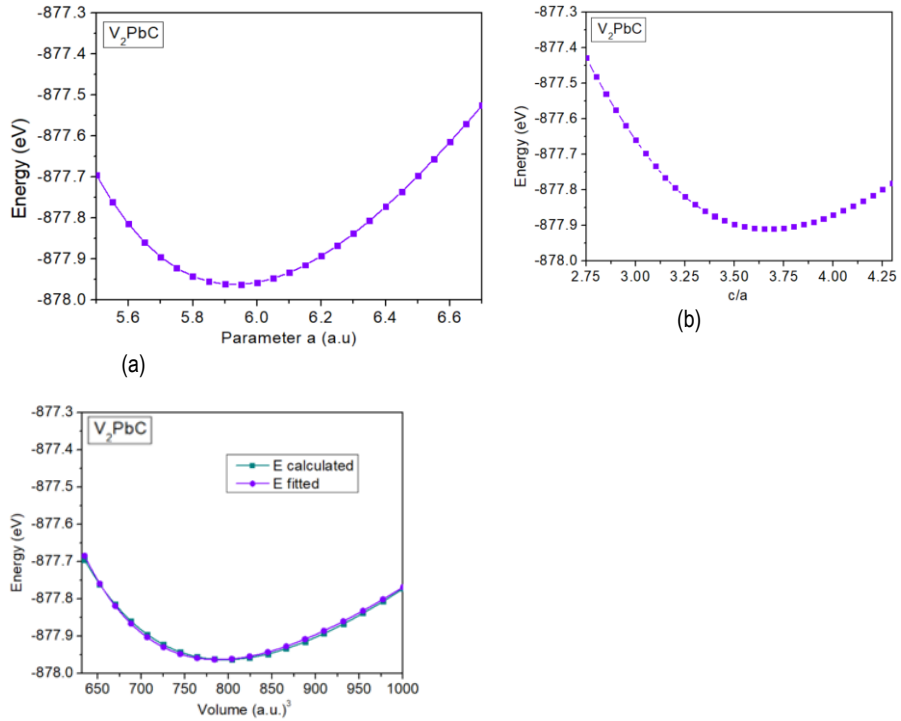

Figure 1: Optimized lattice parameters

The resulting total energy-volume curve in Figure 1(c) was used for calculating the bulk modulus B_0' and its derivative B_0 using the Birch-Murnaghan equation of state, Equation (1) (Hadi et al., 2017; Phatak et al., 2009) to determine the equilibrium primitive cell volume, The optimized structural parameters calculated using the GGA(PBE) are displayed in Table **1**.

$$\boldsymbol{P(V)} = \frac{\boldsymbol{3B_0}}{\boldsymbol{2}}\left[\left(\frac{\boldsymbol{V_0}}{\boldsymbol{V}}\right)^{\frac{7}{3}} - \left(\frac{\boldsymbol{V_0}}{\boldsymbol{V}}\right)^{\frac{5}{3}}\right]\left\{\boldsymbol{1} + \frac{\boldsymbol{3}}{\boldsymbol{4}}\boldsymbol{(B_0' - 4)}\left[\left(\frac{\boldsymbol{V_0}}{\boldsymbol{V}}\right)^{\frac{2}{3}} - \boldsymbol{1}\right]\right\} \quad \textbf{(1)}$$

Table 1. **calculated lattice parameters of a(Å), c(Å), c/a, V$(\text{Å})^3$, bulk modulus B_0'(Gpa) and its derivative B_0, Minimum energy E (Ry)**

MAX Phase	*a*(Å)	*c*(Å)	*c/a*	*V*$(\text{Å})^3$	B_0'	B_0	Min. *E* (Ry)	Ref
V_2PbC	3.240	11.620	3.590	116.70	165.0	5.8	-877.96	This work
V_2SnC	3.121	14.548	4.320	109.2				(Xu et al., 2020)
Hf_2SnC	3.367	14.025	4.219	134.20	141.9			(M. A. Ali & Qureshi, 2021)

Science World Journal Vol. 19(No 3) 2024 https://dx.doi.org/10.4314/swj.v19i3.26
www.scienceworldjournal.org
ISSN: 1597-6343 (Online), ISSN: 2756-391X (Print)
Published by Faculty of Science, Kaduna State University

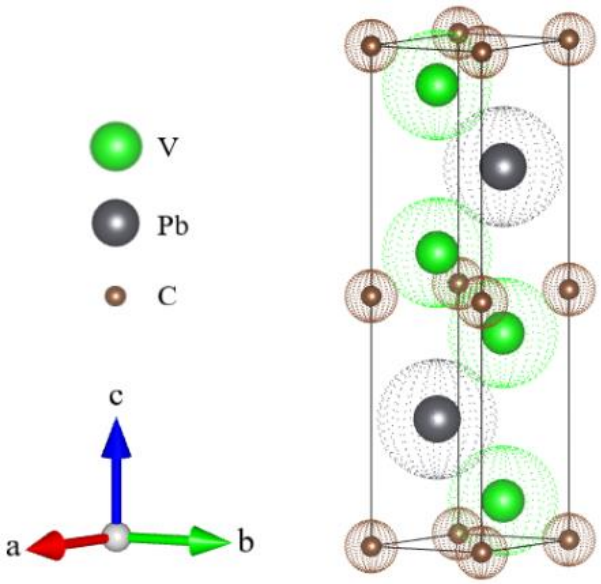

Figure 2: Crystal structure of V_2PbC

Electronic Properties

Figure 3 shows (a) the electronic bands and (b) the total and partial density of states (TDOS and PDOS) calculated along the high symmetry points in the Brillouin zone (BZ) using the equilibrium lattice parameters. It is seen that both valence bands and conduction bands overlap significantly showing there is no energy gap at the Fermi level. This means V_2PbC is metallic, a common behaviour for all MAX compounds. The investigated TDOS) plot for V_2PbC shows that the peaks at and around the fermi are contributions from the V-3d and the Pb-6p orbitals. The TDOS per unit cell at the Fermi level for V_2PbC has been calculated to be 2.27 states/eV. Analysis of bonding properties is obtained from the PDOS of each contributing element where the width of the V-3S state is wider for each one than that of the C-2S state. With several fewer contributing peaks in the V atom due to its 3S states. The V-3S energy states show that there are S-P interactions in V, i.e. close-packed layer V atoms are bonded through S-P interactions. For the energy range -6 eV to +6 eV in the valence bands of V_2PbC, there is a high degree of hybridization of the V-3D, Pb-6P, and C-2P states, which suggests covalent bonding between the orbitals is a driving bonding force in V_2PbC, similar to bonding properties in some 211 MAX phases like Ti_2TlC and Zr_2TlC

Table **1**. The hexagonal structure of MAX phases has six autonomous elastic constants (c_{11}, c_{12}, c_{13}, c_{33}, $c_{44=}c_{55}$ and c_{66}), but five of them are listed since $c_{66} = (c_{11} - 2c_{12})$ (Goldstein et al., 2017).

To comprehend the mechanical properties further, the bulk

Table 2. The Voigt (V)(Liu et al., 2020), Russ (R) (Chung & Buessem, 1968), and Voigt–Russ and Hill (VRH) (Liu et al., 2020) approximations scheme were used to determine the parameters:

(Bouhemadou, 2009b).

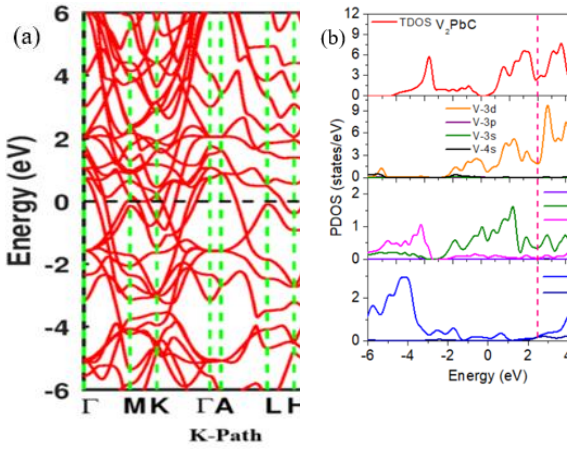

Figure 3: (a)Electronic bands structure, (b) DOS for V_2PbC

Elastic Properties

Elastic constants estimate the response of the crystalline solids to external stresses and measure the strength of the materials. Elastic constants also provide a fundamental insight into the nature of the bonding character between adjacent atomic planes and the anisotropic character of the bonding and structural stability. They can link between a material's dynamical behaviour and its mechanical and thermal properties. For hexagonal MAX phases, five nonzero independent elastic constants, namely c_{11}, c_{12}, c_{13}, c_{33}, and c_{44} are obtained. The elastic constants of V_2PbC fulfills the mechanical stability criteria for hexagonal crystals.

The thermal properties of V_2PbC has been calculated at standard temperature and pressure using a thermo_pw simulation pack(Corso, 2019; Motornyi et al., 2018; Prasad et al., 2019). The Debye temperature (θ_D) is calculated from elastic constants and it depends on the mean propagation sound velocity (v_m). A couple of equations are used to calculate θ_D which are given below(M. S. Ali et al., n.d.). The mechanical stability of V_2PbC was justified by the Born–Huang criteria for a hexagonal crystal as depicted in Equation (2).

$$c_{11} > 0;\ c_{44} > 0; c_{11} > |c_{12}|; (c_{11} + 2c_{12})c_{33} > 2c_{13}^2 \quad (2)$$

A brief knowledge of the elastic constants of a crystalline material helps to predict its
behaviour under the application of external stress. It contributes to a critical understanding of the many solid-state properties, like, ductility, brittleness, stiffness, structural stability, and anisotropy. The mechanical properties of V_2PbC has been calculated and the results are tabulated in
modulus (B), Young's modulus (E), shear modulus (G), G/B or B/G (Pugh ratio), Poisson's ratio (η), and elastic anisotropy (A), are computed from the calculated elastic constants using Equations (5)-(10) and results are given in

$$B = 0.5(B_V + B_R) \quad (3)$$

And

Science World Journal Vol. 19(No 3) 2024 https://dx.doi.org/10.4314/swj.v19i3.26
www.scienceworldjournal.org
ISSN: 1597-6343 (Online), ISSN: 2756-391X (Print)
Published by Faculty of Science, Kaduna State University

$$G = 0.5(G_V + G_R) \quad (4)$$

where B_V, G_V and B_R, G_R are the B and G in terms of the Voigt and Russ approximation respectively and calculated by given Equations (5)-(8)

$$B_V = {}^1/_9\,(2(c_{11} + c_{12}) + 4c_{13} + c_{33}) \quad (5)$$

$$G_V = {}^1/_{30}\,(c_{11} + c_{12} + 2c_{33} - 4c_{13} + 12c_{44} + +12c_{66}) \quad (6)$$

$$B_R = \frac{\left((c_{11} + c_{12})c_{33} - 2c_{12}^2\right)}{(c_{11} + c_{12} + 2c_{33} - 4c_{13})} \quad (7)$$

And

$$G_R = \frac{{}^5/_2\,[((c_{11} + c_{12})\,c_{33} - 2c_{12}^2)^2]c_{55}c_{66}}{\left[3B_V c_{55}c_{66} + \left((c_{11} + c_{12})c_{33} - 2c_{12}^2\right)^2\right](c_{55}+c_{66})} \quad (8)$$

Young's modulus can be calculated by

$$E = \frac{9BG}{3B + G} \quad (9)$$

To calculate the anisotropy index (*A*) the following expression is used.

$$A = \frac{4c_{44}}{c_{11} + c_{33} - 2c_{13}} \quad (10)$$

Table 2 showed V_2PbC is anisotropic with $A = 1.696 > 1$. One of the most essential elastic parameters is Poisson's ratio (σ), defined as the ratio between the transverse strain to longitudinal strain under the applied tensile stress. It gives knowledge about the material's chemical bonding and is linked to

Table 2 shows the mechanical properties of V_2PbC alongside similar 211 MAX phases of V_2SnC, Zr_2PbC, Hf_2SnC. It is seen that the stability conditions of V_2SnC are similar to those of MAX phases, demonstrating its stability under elastic strain perturbations. Besides, the stability of V_2PbC can also be judged from lattice dynamic investigations. As can be seen in the phonon dispersion and phonon density of state curves in Figure 4, all

An anisotropy factor (universal anisotropy index) has recently been proposed for a suitable universal measure of elastic anisotropy of crystals and is denoted as

$$A^U = 5\frac{G_V}{G_R} + \frac{B_V}{B_R} - 6 \quad (11)$$

The Poisson's ratio can be calculated by

$$\eta = \frac{3B - 2G}{2(3B + G)} \quad (12)$$

Generally, the calculated parameters B, G, and E measure the material's resistance to fracture, plastic deformation, and stiffness of the material, respectively. The bulk modulus (B) calculated in terms of elastic constants is in good agreement with the bulk modulus B_0' obtained from the Birch–Murnaghan equation of state (EOS), indicating that our estimated elastic constants for V_2PbC is accurate and precise. Another parameter, the Pugh's ratio (G/B) (M. A. S. Ali et al., 2016; Khatun et al., 2021), separates the ductile to brittle nature of the material. It is known that if B/G > 1.75 and G/B < 0.5, the material will be ductile; else brittle (Zhou et al., 2012). In our cases (V_2PbC), the B/G > 1.75 and G/B < 0.5; consequently, the compound under study is predicted to be ductile. The anisotropy index (A) gives knowledge about the anisotropic nature of the materials. If the value of A is equal to 1 then the material is said to be isotropic; otherwise, the material will be anisotropic if the value of A is higher or lower than 1. Our calculated results from

its stability against the shear stress. Whether a material is brittle or ductile can be predicted from the Poisson's ratio(η) value, and the 0.33 (Bouhemadou, 2009c; Gencer & Surucu, 2018) value is set for ductile material; otherwise, it is brittle if σ < 0.33.

phonon branches are positive, indicating the dynamical stability of this compound against mechanical perturbations. Moreso, for the V_2PbC phase, it is observed that the principal elastic constants c_{11} and c_{33} are larger when compared to all its other c_{ij} for the same material which is clearly common to all the 211 MAX phases.

Table 2: Calculated elastic constants (c_{ij}) bulk modulus (B), Young's modulus (E), shear modulus (G), all in (GPa), Pugh's ratio (B/G and G/B), anisotropic index (A), and Poisson's ratio for V_2PbC

MAX Phase	c_{11}	c_{12}	c_{13}	c_{33}	c_{44}	B	E	G	B/G	G/B	A	η	Ref
V_2PbC	264	155	146	304	117	187	202	85	2.22	0.450	1.696	0.340	This work
V_2SnC	336	126	122	304	85	190	244	95	0.20	0.500	0.859	0.286	(Xu et al., 2020)
Hf_2SnC	330	54	126	292	167	173	316	132	1.31	0.763	1.805	0.195	(Kanoun et al., 2009)

Science World Journal Vol. 19(No 3) 2024 https://dx.doi.org/10.4314/swj.v19i3.26
www.scienceworldjournal.org
ISSN: 1597-6343 (Online), ISSN: 2756-391X (Print)
Published by Faculty of Science, Kaduna State University

Thermodynamic Properties

The thermal properties of V_2PbC has been computed at standard temperature and pressure (STP), The Debye temperature (θ_D), Equation (13) is calculated from elastic constants and it depends on the mean propagation sound velocity (υ_m).

$$\theta_D = {}^{h}/_{k_B}\left[\frac{3n}{4\pi V_a}\right]^{1/3}\upsilon_m \quad (13)$$

$$\upsilon_m = \left[\frac{1}{3}\left(\frac{2}{\upsilon_t^3}+\frac{1}{\upsilon_l^3}\right)\right]^{-1/3} \quad (14)$$

Table 3 depicts the calculated longitudinal elastic (υ_l), transverse elastic (υ_t), and the average (υ_m) velocities(ms^{-1}) and Debye temperature (θ_D) (K), respectively for V_2PbC.

$$\upsilon_t = \left(\frac{G}{\rho}\right)^{1/2} \quad (15)$$

$$\upsilon_l = \left(\frac{3B+4G}{3\rho}\right)^{1/2} \quad (16)$$

where *h* is Planck's constant, k_B is Boltzmann's constant, *n* represents the number of atoms per unit cell V_a is the atomic volume while υ_m, υ_t, and υ_l which have been calculated using Equations (14) - (16) as the longitudinal, transverse, and mean sound velocities respectively.

Table 3. Calculated transverse elastic velocity ($\boldsymbol{\upsilon_t}$), longitudinal elastic velocity ($\boldsymbol{\upsilon_l}$), the average velocity ($\boldsymbol{\upsilon_m}$), ($\boldsymbol{ms^{-1}}$) and Debye temperature ($\boldsymbol{\theta_D}$) ($\boldsymbol{K}$), for $\boldsymbol{V_2PbC}$

MAX Phase	υ_l	υ_t	υ_m	θ_D	Ref
V_2PbC	4340	5402	3087	388	This work
V_2SnC	6.125	3.405	3.792	472	(Hadi et al., 2020)
Hf_2SnC	5228	3113	3446	398.32	(Kanoun et al., 2009)

Phonon Density of States

The stability of V_2PbC can be judged from lattice dynamic investigations. The phase stability of V_2PbC MAX phase, the calculated phonon dispersion curves along the high-symmetry directions in the Brillouin zone are shown in Figure 4. The V_2PbC MAX phases have eight atoms in the unit cell; therefore, the phonon dispersion curve shows twenty-four branches (three acoustic and twenty-one optical). The optical frequencies (longitudinal optical (**LO**) and transverse optical (**TO**)) at **Γ** are $610\ cm^{-1}$ and $820\ cm^{-1}$ for V_2PbC. We have not observed any negative or imaginary frequency in the phonon dispersion curves of the nanolaminate, which means all phonon branches are positive, indicating the presence of dynamical stability in V_2PbC MAX phase against mechanical perturbations. As there are no works of literature on phonon properties of V_2PbC for comparison, our results can be compared to those of similar works on 211 MAX phases in literature.

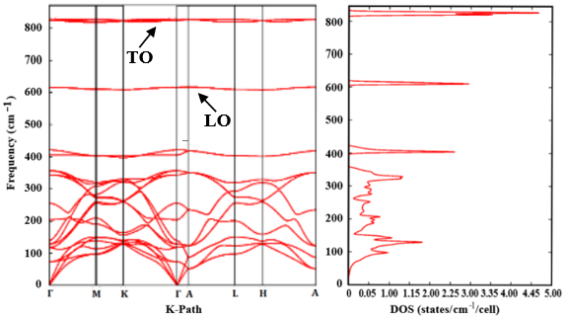

Figure 4: Calculated phonon dispersion relations of V_2PbC

Conclusion

The structural, electronic, elastic, thermodynamic, and phonon properties of stable V_2PbC MAX phase has been investigated. Calculated energy bands and DOS(2.252 states/eV) reveal that the main contribution to conduction properties at the Fermi, E_F level is due to the hybridizations between V-3d and Pb-6p states. Calculated elastic constants and phonon properties show the compound is brittle, stable, and anisotropic. Our results can serve as a reference for future theoretical and experimental research on V_2PbC.

Acknowledgments

This research is sponsored by TETFund through the Institution-Based Research (IBR) TETF/DR&D/UNI/MUBI/RG/2023/VOL.1

REFERENCES

Ali, M. A., & Qureshi, M. W. (2021). Newly synthesized MAX phase Zr_2SeC: DFT insights into physical properties towards possible applications. *RSC Advances*, *11*(28), 16892–16905. https://doi.org/10.1039/D1RA02345D

Ali, M. A. S., Ali, M. A. S., & Uddin, M. M. (2016). Structural, elastic, electronic and optical properties of metastable MAX phase Ti_5SiC_4 compound. *Indian Journal of Pure and Applied Physics*, *54*(6), 386–390. http://op.niscair.res.in/index.php/IJPAP/article/view/4502

Ali, M. S., Islam, A. K. M. A., Hossain, M. M., & Parvin, F. (n.d.). *Phase stability , elastic , electronic , thermal and optical properties of $Ti_3Al_{1-x}Si_xC_2$ ($0 \le x \le 1$): First principle study*. *2*, 1–13.

Anasori, B., Dahlqvist, M., Halim, J., Moon, E. J., Lu, J., Hosler, B. C., Caspi, E. N., May, S. J., Hultman, L., Eklund, P., Rosén, J., & Barsoum, M. W. (2015). Experimental and theoretical characterization of ordered MAX phases Mo2TiAlC2 and Mo2Ti2AlC3. *Journal of Applied Physics*, *118*(9), 094304. https://doi.org/10.1063/1.4929640

Azzouz-Rached, A., Rached, H., Ouadha, I., Rached, D., & Reggad, A. (2021). The Vanadium-doping effect on physical properties of the Zr_2AlC MAX phase compound. *Materials Chemistry and Physics*, *260*(September 2020), 124189.

https://doi.org/10.1016/j.matchemphys.2020.124189

Barsoum, M. (2014). *The MAX Phases : Unique New Carbide and Nitride Materials*. *November*. https://doi.org/10.1511/2001.28.736

Bouhemadou, A. (2008). Calculated structural and elastic properties of M_2InC (M = Sc, Ti, V, Zr, Nb, Hf, Ta). *Modern Physics Letters B*, *22*(22), 2063–2076. https://doi.org/10.1142/S0217984908016807

Bouhemadou, A. (2009a). *First-principles study of structural , electronic and elastic properties of Nb_4AlC_3*. 52–57.

Bouhemadou, A. (2009b). Structural, electronic and elastic properties of Ti2TlC, Zr2TlC and Hf2TlC. *Central European Journal of Physics*, *7*(4), 753–761. https://doi.org/10.2478/s11534-009-0022-z

Bouhemadou, A. (2009c). Structural, electronic and elastic properties of Ti_2TlC, Zr_2TlC and Hf_2TlC. *Central European Journal of Physics*, *7*(4), 753–761. https://doi.org/10.2478/s11534-009-0022-z

Bouhemadou, A. (2010). First-principles study of structural, electronic and elastic properties of Nb_4AlC_3. *Brazilian Journal of Physics*, *40*(1), 52–57. https://doi.org/10.1590/S0103-97332010000100009

Chlubny, L., Lis, J., Chabior, K., Chachlowska, P., & Kapusta, C. (2015). Processing and properties of max phases-Based materials using SHS technique. *Archives of Metallurgy and Materials*, *60*(2A), 859–863. https://doi.org/10.1515/amm-2015-0219

Choudhary, K., & Tavazza, F. (2019). Convergence and machine learning predictions of Monkhorst-Pack k-points and plane-wave cut-off in high-throughput DFT calculations. *Computational Materials Science*, *161*, 300–308. https://doi.org/10.1016/j.commatsci.2019.02.006

Chung, D. H., & Buessem, W. R. (1968). The voigt-reuss-hill (vrh) approximation and the elastic moduli of polycrystalline zno, tio2 (rutile), and α-al2o 3. *Journal of Applied Physics*, *39*(6), 2777–2782. https://doi.org/10.1063/1.1656672

Corso, D. (2019). *Temperature-dependent atomic B factor : an ab initio calculation research papers*. *1996*, 624–632. https://doi.org/10.1107/S205327331900514X

Dal, A., & Sissa, C. (n.d.). *Thermo pw : Thermodynamics of crystals*.

Dal Corso, A. (2016). Elastic constants of beryllium: A first-principles investigation. *Journal of Physics Condensed Matter*, *28*(7). https://doi.org/10.1088/0953-8984/28/7/075401

Dove, M. (2003). Oxford master series in condensed matter physics. *Oxford University Press*, 334.

Eklund, P., Beckers, M., Jansson, U., Högberg, H., & Hultman, L. (2010). The $M_{n+1}AX_n$ phases: Materials science and thin-film processing. *Thin Solid Films*, *518*(8), 1851–1878. https://doi.org/10.1016/j.tsf.2009.07.184

Fischer, T. H., & Almlöf, J. (1992). General methods for geometry and wave function optimization. *Journal of Physical Chemistry*, *96*(24), 9768–9774. https://doi.org/10.1021/j100203a036

Gencer, A., & Surucu, G. (2018). Electronic and lattice dynamical properties of Ti2SiB MAX phase. *Materials Research Express*, *5*(7). https://doi.org/10.1088/2053-1591/aace7f

Goldstein, R. V, Gorodtsov, V. A., Komarova, M. A., & Lisovenko, D. S. (2017). Scripta Materialia Extreme values of the shear modulus for hexagonal crystals. *Scripta Materialia*, *140*, 55–58. https://doi.org/10.1016/j.scriptamat.2017.07.002

Gupta, S., Hoffman, E. N., & Barsoum, M. W. (2006). Synthesis and oxidation of Ti_2InC, Zr_2InC, $(Ti_{0.5},Zr_{0.5})2InC$ and $(Ti_{0.5},Hf_{0.5})_2InC$ in air. *Journal of Alloys and Compounds*, *426*(1–2), 168–175. https://doi.org/10.1016/j.jallcom.2006.02.049

Hadi, M. A., Dahlqvist, M., Christopoulos, S. R. G., Naqib, S. H., Chroneos, A., & Islam, A. K. M. A. (2020). Chemically stable new MAX phase V2SnC: A damage and radiation tolerant TBC material. *RSC Advances*, *10*(71), 43783–43798. https://doi.org/10.1039/d0ra07730e

Hadi, M. A., Roknuzzaman, M., Chroneos, A., Naqib, S. H., Islam, A. K. M. A., Vovk, R. V., & Ostrikov, K. (2017). Elastic and thermodynamic properties of new $(Zr_{3-x}Ti_x)AlC_2$ MAX-phase solid solutions. *Computational Materials Science*, *137*, 318–326. https://doi.org/10.1016/j.commatsci.2017.06.007

Ingason, A. S., Petruhins, A., Dahlqvist, M., Magnus, F., Mockute, A., Alling, B., Hultman, L., Abrikosov, I. A., Persson, P. O. Å., & Rosen, J. (2017). A nanolaminated magnetic phase: Mn_2GaC. *Materials Research Letters*, *2*(2), 89–93. https://doi.org/10.1080/21663831.2013.865105

Istomin, P., Istomina, E., Nadutkin, A., Grass, V., & Presniakov, M. (2016). Synthesis of a Bulk Ti4SiC3 MAX Phase by Reduction of TiO2 with SiC. In *Inorganic Chemistry* (Vol. 55, Issue 21, pp. 11050–11056). https://doi.org/10.1021/acs.inorgchem.6b01601

Kanoun, M. B., Goumri-said, S., & Reshak, A. H. (2009). *Theoretical study of mechanical , electronic , chemical bonding and optical properties of Ti_2SnC, Zr_2SnC, Hf_2SnC and Nb_2SnC*. *47*, 491–500. https://doi.org/10.1016/j.commatsci.2009.09.015

Khatun, R., Rahman, M. A., Hossain, K. M., Hasan, M. Z., Rasheduzzaman, M., & Sarker, S. (2021). Physical properties of MAX phase Zr2PbC under pressure: Investigation via DFT scheme. *Physica B: Condensed Matter*, *620*(July), 413258. https://doi.org/10.1016/j.physb.2021.413258

Khazaei, M., Arai, M., Sasaki, T., Chung, C.-Y., Venkataramanan, N. S., Estili, M., Sakka, Y., & Kawazoe, Y. (2013). Novel Electronic and Magnetic Properties of Two-Dimensional Transition Metal Carbides and Nitrides. *Advanced Functional Materials*, *23*(17), 2185–2192. https://doi.org/10.1002/adfm.201202502

Khazaei, M., Arai, M., Sasaki, T., Estili, M., & Sakka, Y. (2014). The effect of the interlayer element on the exfoliation of layered Mo_2AC (A = Al, Si, P, Ga, Ge, As or In) MAX phases into two-dimensional Mo_2C nanosheets. *Science and Technology of Advanced Materials*, *15*(1). https://doi.org/10.1088/1468-6996/15/1/014208

Khazaei, M., Ranjbar, A., Arai, M., Sasaki, T., & Yunoki, S. (2017). Electronic properties and applications of MXenes: a theoretical review. *Journal of Materials Chemistry C*, *5*(10), 2488–2503. https://doi.org/10.1039/c7tc00140a

Kucukbenli, E., Monni, M., Adetunji, B. I., Ge, X., Adebayo, G. A., Marzari, N., de Gironcoli, S., & Corso, A. D. (2014). *Projector augmented-wave and all-electron calculations across the periodic table: a comparison of structural and energetic properties*. http://arxiv.org/abs/1404.3015

Recent advances in MXene Preparation properties, (2015). https://doi.org/10.1007/s11467-015-0493-x

Li, Y. F., Ding, Y. C., Xiao, B., & Cheng, Y. H. (2016). Anisotropic electrical and lattice transport properties of ordered quaternary phases Cr_2TiAlC_2 and Mo_2TiAlC_2: A first principles study. *Physics Letters, Section A: General, Atomic and Solid State Physics*, *380*(44), 3748–3755. https://doi.org/10.1016/j.physleta.2016.09.015

Liu, C., Liu, Z., Ye, X., Cheng, P., & Li, Y. (2020). First-principles study of structural, elastic and electronic properties of naphyne and naphdiyne. *RSC Advances*, *10*(58), 35349–35355. https://doi.org/10.1039/d0ra07214a

Malica, C., & Dal Corso, A. (2019). Temperature-dependent atomic B factor: An ab initio calculation. *Acta Crystallographica Section A: Foundations and Advances*, *75*(1996), 624–632. https://doi.org/10.1107/S205327331900514X

Motornyi, O., Raynaud, M., Dal Corso, A., & Vast, N. (2018). Simulation of electron energy loss spectra with the turboEELS and thermo-pw codes. *Journal of Physics: Conference Series*, *1136*(1). https://doi.org/10.1088/1742-6596/1136/1/012008

Pack, H. J. M. and J. D. (1976). Special points for Brillonin-zone integrations. *Physical Review B*, *13*(12), 1748–1749.

Pack, J. D., & Monkhorst, H. J. (1977). "Special points for Brillouin-zone integrations"—a reply. *Physical Review B*, *16*(4), 1748–1749. https://doi.org/10.1103/PhysRevB.16.1748

Payne, M. C., Teter, M. P., Allan, D. C., Arias, T. A., & Joannopoulos, J. D. (1992). Iterative minimization techniques for ab initio total-energy calculations: Molecular dynamics and conjugate gradients. *Reviews of Modern Physics*, *64*(4), 1045–1097. https://doi.org/10.1103/RevModPhys.64.1045

Perdew, J. P., Burke, K., & Ernzerhof, M. (1996). Generalized Gradient Approximation Made Simple. *Phys. Rev. Lett*, *77*(18), 3865–3868.

Phatak, N. A., Saxena, S. K., Fei, Y., & Hu, J. (2009). Synthesis and structural stability of Ti2GeC. *Journal of Alloys and Compounds*, *474*(1–2), 174–179. https://doi.org/10.1016/j.jallcom.2008.06.073

Prasad, T., Shah, M., Singh, P., & Wani, T. A. (2019). Ab-initio Calculations of Properties for NbB_2 Under High-Pressure Using Quantum ESPRESSO. *SSRN Electronic Journal*, *figure 1*, 836–843. https://doi.org/10.2139/ssrn.3355175

Qian, X. K., Wu, H. Y., Zhu, H. P., Ma, S. H., & Jiang, T. (2016). First-principles study of a new higher-order max phase of $Ti_5Al_2C_3$. *Journal of Ceramic Science and Technology*, *7*(1), 47–52. https://doi.org/10.4416/JCST2015-00027

Sobolev, K., Pazniak, A., Shylenko, O., & Gryń, A. M.-. (2017). *Magnetic Properties of Highly Pure (Cr 1-x Mn x) 2 AlC MAX-Phase*. *28*(2000), 236041.

Surucu, G., Colakoglu, K., Deligoz, E., & Korozlu, N. (2016). *First-Principles Study on the MAX Phases $Ti_{n+1}GaN_n$ (n = 1, 2, and 3)*. https://doi.org/10.1007/s11664-016-4607-1

Wu, S., Dimakis, A. G., Sanghavi, S., Yu, F. X., Holtmann-Rice, D., Storcheus, D., Rostamizadeh, A., & Kumar, S. (2018). *The Sparse Recovery Autoencoder*. 455–465. https://doi.org/10.1007/978-981-10-2134-3

Xu, Q., Zhou, Y., Zhang, H., Jiang, A., Tao, Q., Lu, J., Rosén, J., Niu, Y., Grasso, S., & Hu, C. (2020). Theoretical prediction, synthesis, and crystal structure determination of new MAX phase compound V2SnC. *Journal of Advanced Ceramics*, *9*(4), 481–492. https://doi.org/10.1007/s40145-020-0391-8

Yang, T., Wang, C., Liu, W., Liu, S., Xiao, J., Huang, Q., Xue, J., Yan, S., & Wang, Y. (2017). Formation of nano-twinned structure in Ti_<3/AlC>/_2 induced by ion-irradiation. *Acta Materialia*, *128*, 1–11. https://doi.org/10.1016/j.actamat.2017.01.066

Zhan, X., Si, C., Zhou, J., & Sun, Z. (2020). MXene and MXene-based composites: Synthesis, properties and environment-related applications. *Nanoscale Horizons*, *5*(2), 235–258. https://doi.org/10.1039/c9nh00571d

Zhou, L., Holec, D., & Mayrhofer, P. (2012). First-principles study of elastic properties of Cr-Al-N. *ArXiv Preprint ArXiv:1209.0955*, 1–24. https://doi.org/10.1063/1.4793084